Ecotoxicology and Environmental Safety 271 (2024) 115981

Contents lists available at ScienceDirect

Ecotoxicology and Environmental Safety

journal homepage: www.elsevier.com/locate/ecoenv

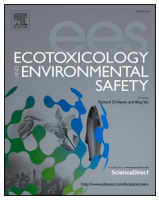

Accelerated fragmentation of two thermoplastics (polylactic acid and polypropylene) into microplastics after UV radiation and seawater immersion

Zhiyue Niu [a,b,*], Marco Curto [c], Maelenn Le Gall [d], Elke Demeyer [e], Jana Asselman [b], Colin R Janssen [b,2], Hom Nath Dhakal [c], Peter Davies [d], Ana Isabel Catarino [a,1], Gert Everaert [a,1]

[a] Flanders Marine Institute (VLIZ), InnovOcean Campus, Jacobsenstraat 1, 8400 Oostende, Belgium
[b] Blue Growth Research Lab, Ghent University, Bluebridge Building, Ostend Science Park 1, 8400 Ostend, Belgium
[c] Advanced Polymers and Composites (APC) Research Group, School of mechanical and Design Engineering, University of Portsmouth, Portsmouth PO1 3DJ, UK
[d] Marine Structures Laboratory, IFREMER, Centre de Bretagne, 29280, France
[e] Functional Thermoplastic Textiles, Centexbel, Industriepark Zwijnaarde 70, 9052 Gent, Belgium

ARTICLE INFO

Original content: Microplastics formation data on polylactic acid and polypropylene items after UV radiation and seawater immersion (Original data)

Keywords:
Fragmentation
Microplastics formation
Bio-based plastics
Polylactic acid
Ultraviolet radiation
Polypropylene

ABSTRACT

To better understand the fate and assess the ingestible fraction of microplastics (by aquatic organisms), it is essential to quantify and characterize of their released from larger items under environmental realistic conditions. However, the current information on the fragmentation and size-based characteristics of released microplastics, for example from bio-based thermoplastics, is largely unknown. The goal of our work was to assess the fragmentation and release of microplastics, under ultraviolet (UV) radiation and in seawater, from polylactic acid (PLA) items, a bio-based polymer, and from polypropylene (PP) items, a petroleum-based polymer. To do so, we exposed pristine items of PLA and PP, immersed in filtered natural seawater, to accelerated UV radiation for 57 and 76 days, simulating 18 and 24 months of mean natural solar irradiance in Europe. Our results indicated that 76-day UV radiation induced the fragmentation of parent plastic items and the microplastics (50 - 5000 μm) formation from both PP and PLA items. The PP samples (48 ± 26 microplastics / cm^2) released up to nine times more microplastics than PLA samples (5 ± 2 microplastics / cm^2) after a 76-day UV exposure, implying that the PLA tested items had a lower fragmentation rate than PP. The particles' length of released microplastics was parameterized using a power law exponent (α), to assess their size distribution. The obtained α values were 3.04 ± 0.11 and 2.54 ± 0.06 (-) for 76-day UV weathered PP and PLA, respectively, meaning that PLA microplastics had a larger sized microplastics fraction than PP particles. With respect to their two-dimensional shape, PLA microplastics also had lower width-to-length ratio (0.51 ± 0.17) and greater fiber-shaped fractions (16%) than PP microplastics (0.57 ± 0.17% and 11%, respectively). Overall, the bio-based PLA items under study were more resistant to fragmentation and release of microplastics than the petroleum-based PP tested items, and the parameterized characteristics of released microplastics were polymer-dependent. Our work indicates that even though bio-based plastics may have a slower release of fragmented particles under UV radiation compared to conventional polymer types, they still have the potential to act as a source of microplastics in the marine environment, with particles being available to biota within ingestible size fractions, if not removed before major fragmentation processes.

1. Introduction

Bio-based plastics, originating from natural feedstocks, such as polylactic acid (PLA), are gaining interest as alternatives to conventional plastics (produced from petroleum derivatives) (Curto et al., 2021), but little is known about their potential as a source of microplastics

* Corresponding author at: Flanders Marine Institute (VLIZ), InnovOcean Campus, Jacobsenstraat 1, 8400 Oostende, Belgium.
E-mail address: zhiyue.niu@vliz.be (Z. Niu).
[1] Authors had an equal contribution and share senior authorship.
[2] ORCID: https://orcid.org/0000-0002-7781-6679

https://doi.org/10.1016/j.ecoenv.2024.115981
Received 22 September 2023; Received in revised form 19 December 2023; Accepted 12 January 2024

pollution in the marine environment. Microplastics are plastic particles with sizes between 1 μm and 5 mm, which have been observed in most of the marine ecosystems (SAPEA, 2019). Apart from intentionally manufactured microbeads (primary), most microplastics (secondary) in the marine environment are fragmented from larger-sized plastics (SAPEA, 2019). Due to the small dimensions of microplastics, they can be (bio) accessible to aquatic organisms, as their dimensions are within the size fraction of their prey, and can induce adverse effects (Everaert et al., 2022). To date, only a few studies have reported the occurrence of bio-based microplastics in the environment (Okoffo et al., 2022), probably mostly due to their short application history and limited production (European Bioplastics, 2021), but possibly also due to current methodological constrains (Okoffo et al., 2022). Therefore, to better understand the potential environmental fate of bio-based microplastics (Alexy et al., 2020), there is a need of information on the fragmentation of larger-sized bio-based plastics and characteristics of these fragments, compared to common petroleum-based plastics, under simulated marine environment.

Ultraviolet (UV) radiation from sunlight is one of the main stressors that induces plastic fragmentation and the formation of microplastics (Ter Halle et al., 2016). Most thermoplastics, including several bio-based polymers such as PLA, can undergo a photochemical reaction to absorb UV radiation, which induces cleavage of C–C and C–H bonds, release of free radicals and subsequently the formation of carbonyl (C═O) groups (Gewert et al., 2015; Curto et al., 2021). As a consequence, the surface of plastics becomes brittle where cracks and groove textures steadily develop, and microplastics can be formed and released (Ter Halle et al., 2016). Laboratory studies have reported the fragmentation and release of microplastics from macro-sized plastic items, of several conventional petroleum-based polymers after accelerated artificial UV radiation (Song et al., 2022). However, only a few studies focused on the fragmentation and release of microplastics from bio-based plastics such as PLA, especially under simulated marine conditions, i.e., in seawater, where their biodegradation is low (SAPEA, 2020). In one of the few reports of microplastics formation from bio-based plastics, Le Gall et al. (2022) have observed that similar concentrations of PLA microplastics (2.2 microplastics / cm^2, 50 – 5000 μm) were released in samples subject to 38-day exposure to UV radiation (equivalent to 12-month mean sunlight radiation in Europe) while immersed in seawater. Each of these studies increased our quantitative knowledge of the concentrations of microplastics released from bio-based plastics after in the marine environment, as an estimate of fragmentation. However, with the increasing interest of replacing conventional plastics with PLA and other bio-based plastics in the marine applications (Curto et al., 2021), the assessment of both the fragmentation of the materials, but also on the characteristics of the released particles is critical to understanding the (bio)accessibility of the particles for ingestion by organisms.

Microplastics released resulting from fragmentation consists of a complex, diverse mixture of particles with different sizes and shapes. These characteristics can not only indicate the patterns of fragmentation but are also relevant to their potential (bio)accessibility to organisms via ingestion. For example, only microplastics smaller than the mouth size can be ingested (Koelmans et al., 2020), and fiber-shaped microplastics, with a longer gut retention time (Au et al., 2015), are considered more harmful than particle-shaped microplastics (Ziajahromi et al., 2017). Thus, a better parameterization of the characteristics of released microplastics is needed to establish a link between their potential environmental fate and exposure pathways to aquatic organisms. According to Cózar et al. (2014) and Kaandorp et al. (2021), the size distribution of microplastics resulting from fragmentation follows a power law shape curve with a negative exponent (-α), whose magnitude is determined by the degree of fragmentation. For example, an α value of less than 2.67 suggests that microplastic fragments are directly released from the parent plastic item, while α equal to or greater than 2.67 indicates the occurrence of cascading fragmentation of released microplastics, i.e., the released fragments break down into even smaller pieces (Kaandorp et al., 2021). For microplastics in the aquatic environment, the mean α usually varies between 2.5 (polyethylene) and 3.3 (polyethylene-chlorinate) by polymers. In addition to being a statistical parameter useful in the characterization of microplastics released from larger materials, it also has direct policy implications as it is related to a more realistic risk assessment (Koelmans et al., 2020). Based on the power law exponent, abundance data of released bio-and petroleum--based microplastics can be rescaled into (bio)accessible fractions for different species, to support a sound environmental risk assessment of bio-based microplastics (Koelmans et al., 2020).

The goal of the present study was to compare, quantify and characterize the microplastics formation from plastic items of PLA (a bio-based polymer) and PP (a petroleum-based polymer, as a benchmark assessment) after exposure to UV radiation while immersed in seawater. To do so, we exposed three-dimensional (3D) printed items of PLA and PP respectively, immersed in filtered natural seawater, to accelerated artificial UV radiation for 57 and 76 days, simulating 18 and 24 months of mean natural solar exposure in Europe (Gewert et al., 2018). The fragmentation and microplastics release from both polymers were assessed using three key parameters: (1) abundance, i.e., number of released microplastics per surface area of parent plastic items, to estimate fragmentation; (2) distribution of particles' length and shape, to assess their two-dimensional particle characteristics; and (3) oxidation status, using the carbonyl index as a proxy (Beltrán-Sanahuja et al., 2020; Simon-Sánchez et al., 2022). The parent plastic items used in the weathering experiment were inspected for changes in surface morphology and oxidation resistance, as an indication of their weathering status.

2. Materials and methods

2.1. Materials

Polylactic acid (PLA) and Polypropylene (PP) filaments were obtained within the SeaBioComp project (Interreg 2 Seas, 2019–2023). Three-dimensional cylinders (d = h = 1 cm, nominal total surface area = 4.7 cm^2) were printed using these filaments at the University of Portsmouth (UK). The advantage of using 3D-pritning cylindrical samples is that they have regular and fine surfaces (Fig. 1). Both PLA and PP items were stored at 22 ± 1 °C in the dark before testing. Natural seawater (salinity ≈ 34 PSU) was pumped from the port of Ostend (Belgium) and filtered through a 0.22 μm Sterivex™ filter prior to use.

2.2. Accelerated Ultraviolet (UV) exposure

Plastic items were exposed to UV in a weathering chamber (Atlas Suntest CPS+) fitted with a Xenon lamp (ISO, 2006) (1500 W) and daylight filter, with wavelength regulated at 300 - 400 nm. Irradiation intensity was conducted at 60 W / m^2 and temperature in the chamber was maintained at 33 ± 3 °C (Black standard temperature = 50 °C). The inner surface of the weathering chamber was coated with UV and light mirrors allowing specimens to receive radiation from all directions. Prior to exposure, items were gently rinsed with Milli-Q water (Millipore Corporation). Each cylinder was placed in a pre-cleaned 25 mL quartz cuvette, as glass partially blocks UV radiation, and immersed with 20 mL filtered natural seawater (Section 2.1). The initial water level in each cuvette was marked to monitor possible water evaporation. The loss of water through evaporation was compensated by adding Milli-Q water (Millipore Corporation) every three weeks. For each polymer, six replicate samples were taken after 57 and 76 days, which corresponded to 18 and 24 months of central European solar irradiance exposure, respectively (Sørensen et al., 2021). Dark control samples (6 replicates), which were cuvettes wrapped in aluminum foil to block radiation, were incubated under the same conditions at the same time in the same UV weathering chamber. Six replicates of sealed cuvettes were incubated in the chamber only for 10 min to account for microplastics

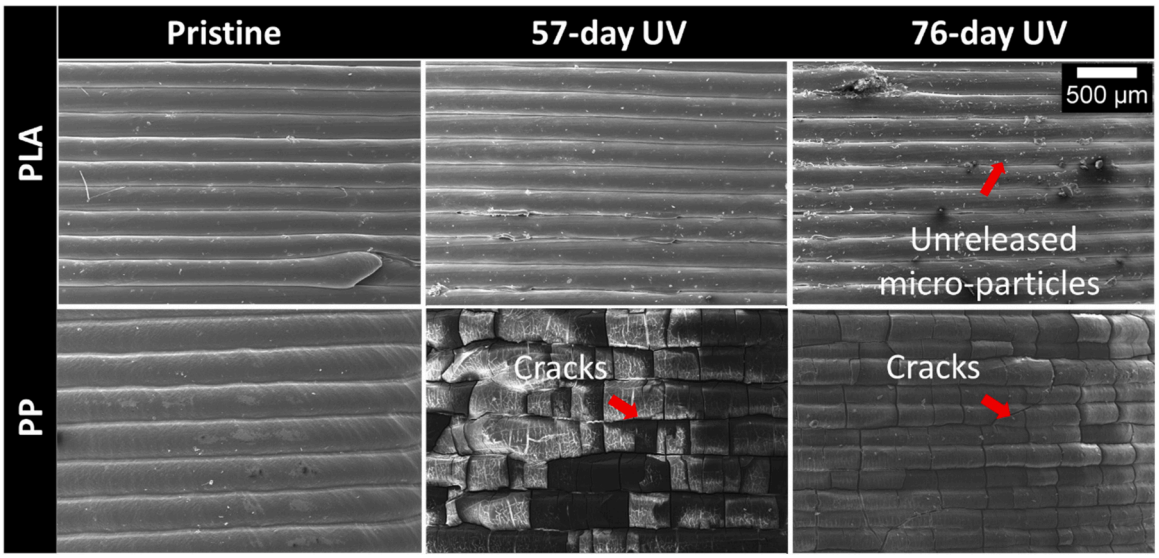

Fig. 1. Scanning electron microscopy (SEM) images of PP and PLA items exposed to UV for 57 and 76 days, compared to pristine samples. Images shown here were captured at 100 × magnification using a 10 mm working distance and a 2 – 10 kV accelerating voltage. Cracks (white) and unreleased micro-particles (white) are marked on the images with red arrows.

release in pristine samples.

To extract microplastics, water samples were filtered through 10 μm polytetrafluoroethylene (PTFE) membrane filters, stained for 15 min with 1 mL Nile red [10 μg / mL in acetone; based on Meyers et al. (2022)]. Then the filters were stored in glass petri-dishes at room temperature in the dark until dry, for further microplastics analysis. A procedural blank (20 mL Milli-Q water) was performed prior to testing each sample to account for background contamination of PLA and PP. Items were also collected and stored in glass vials at 22 ± 1 °C in the dark until dry, for further analysis.

2.3. Microplastics analysis

To identify, quantify and characterize the microplastics released from the PLA and PP items, we used a combination of fluorescent microscopy, infrared techniques, and image analysis.

2.3.1. Fluorescent microscopy and photo-acquisition

All fluorescence microscopy was performed using a Leica DM1000 LED fluorescent microscope (10 x objective lens) connected with a separate beam path. Manual measurements of particles' length (μm) and photo acquisition were performed using a Leica camera and the software LAS Core™ (Leica). Filter samples, after drying, were observed under two fluorescence filters (Leica): blue (BL, Filter System I3 S, BP 450–490 nm) and ultraviolet (UV, Filter System A S, Band Pass (BP) 340–380 nm), to visually identify either PLA or PP microplastics. According to our previous work (Le Gall et al., 2022), the PLA microplastics were yellow / orange (observed through ocular lens, here and after) under both UV and BL fluorescence filters, while PP microplastics were transparent under UV filter and yellow under BL filter (Fig. S1). To avoid color distortion during observations, the work was performed in a dark environment, and the white balance was first set, in bright field mode, in a membrane filter position with no particles. All visually identified PLA and PP microplastics with a length over 45 μm, measured on their longest dimension using the annotation bar in the software LAS Core™ (Leica Application Suite version 4.13.0), were photographed under the BL fluorescence filter for further image analysis. Default software settings for image acquisition were: gain: 1.0x; saturation: 1.50; and gamma: 0.60. As per Meyers et al. (2022), to avoid insufficient or over-exposure, images were captured at exposure times between 2.91 and 12.5 ms for BL filter, while the actual values were selected based on the fluorescence intensity of particles. Microplastics with lengths which exceeded the scale of images (fiber-shape; 1200 - 5000 μm) were counted, but no photos were taken. The particles' polymer composition was further confirmed by analyzing 10% of the visually identified PLA and PP microplastics on each membrane filter sample, in a total 280 out of 3386 particles. The selected sub-samples were randomly inspected using micro-Fourier-transform-infrared spectroscopy (μFTIR, for detailed measurement parameters, see section 2.3.3).

2.3.2. Image analysis

Images of microplastics from each filter sample were processed in batch using a macro script developed by the authors in ImageJ (Schindelin et al., 2012). In this image recognition step, each image imported into ImageJ (Schindelin et al., 2012) was converted to 16-bit grayscale and microplastics in each image were selected from the background by manually adjusting the color threshold. For each particle, minimum and maximum Feret's diameters, i.e., the minimum and maximum distance between two perpendicular tangents of the particle (Sandler and Wilson, 2010), were measured (accuracy up to 1 μm). After the measurements, all selected particles were labeled and the data of particles smaller than 50 μm in their maximum Feret's diameter were removed prior to exporting the dataset. In rare cases (57 out of 3386 particles, < 2%), the color threshold of the particles could not be properly determined, and these particles were then only used for enumeration, but no size was measured.

2.3.3. μFTIR analysis

A Fourier transform infrared (FTIR) spectrometer with a μ-FTIR microscope Spotlight 200i (Frontier, PerkinElmer, Zaventem, Belgium) was used to confirm the polymer characterization of 10% of the visually identified PLA and PP particles. All particles were analyzed with a magnification of 10x, and the detector type was liquid nitrogen-cooled mercury cadmium telluride. Beam splitter OptKBr and mid-infrared (MIR) source set the infrared spectral range of 4000 - 600 cm^{-1}. All spectra were recorded in transmittance mode with a resolution of 4 cm^{-1} with an average of 64 scans per particle. The aperture size changed relative to the size of the particle being measured (dimensions: maximum 100 ×100 μm, minimum 20 ×20 μm). Once a particle was scanned in transmission, a spectrum was produced, and a search was carried out on the spectrum for particle comparison from various commercial libraries (PerkinElmer) such as POLIMERI and FIBERS3. Since

weathering of microplastics affects their spectra (Simon et al., 2021), and that these libraries only include data of pristine plastics, a minimum match score of 60% instead of 70% was selected for determining the polymer composition of released particles. The polytetrafluoroethylene (PTFE) filters that supported the microplastics samples have a high absorption in the range of 1250 – 1150 cm^{-1}, so this range was excluded when carrying out the library search, so not to interfere with the spectra identification.

2.4. Weathered and control plastic items

2.4.1. Scanning electron microscopy (SEM) observation

Changes in the surface morphology of pristine, UV-weathered and dark control samples were visually inspected by scanning electron microscopy (SEM). Items were lightly coated under vacuum, with a 1 nm thick gold-palladium coating using a rotary pumped coater (Quorum Q150 R-S). Surfaces of retrieved plastic items were inspected from top and side on a SEM (ZEISS EVO MA10). Images were captured at magnifications of 40 and 500 × using a 10 mm working distance and a 2–10 kV accelerating voltage.

2.4.2. Oxidation induction time measurement

The oxidation resistance of retrieved plastic items was measured by differential scanning calorimetry (DSC) on a Discovery DSC 25 equipment (TA Instrument). The measurements were carried out in isothermal mode according to ISO 11357–6 (ISO, 2018). The oxidation induction time (OIT) was selected as the parameter of oxidation resistance and determined as the time (minutes) to the onset of oxidation during heating in an oxygen environment (McKeen, 2014). A decrease in OIT value indicates the impeded oxidation resistance, and typically an OIT of 0 min means the loss of all oxidation resistance (McKeen, 2014). The test temperature started at 50 °C and increased with a heating ramp of 10 °C / minute until an isothermal temperature reached. The isothermal temperature was 200 °C for PP and 230 °C for PLA.

2.5. Data analysis and statistics

2.5.1. Particles' length and shape of released microplastics

We used two-dimensional images to characterize particles' size and shape of released microplastics after UV exposure at treatment levels 57-day and 76-day UV exposure, for each polymer type. To do so, we used the particle's maximum and minimum Feret's diameter (μm) measured from the image analysis (section 2.3.2), as the proxy of particles' length and width, respectively and their ratio (W: L), as the proxy of their two-dimensional shape (Simon et al., 2018). Considering that the shape category is commonly reported in microplastics research (Hartmann et al., 2019), "fiber-shape" were identified as microplastics ($\geq$ 50 μm) with a width-to-length ratio $\leq$ 0.33 (Simon et al., 2018), while the rest were categorized as "particle-shape". Cumulative frequency distributions of these three parameters were plotted for UV-exposed samples of both PLA and PP. Particles' length were fitted into a probability density function on treatment level following the method by Kooi et al. (2021). According to earlier theoretical studies [e.g. McDowell and Bolton (1998)], the size distribution of particles as a result of fragmentation follow a power law shape, thus the same are expected for the released microplastics in the present study. According to Kooi et al. (Kooi et al., 2021), the power law exponent was estimated using the maximum likelihood estimation (MLE) method (Clauset et al., 2009). The minimum particles' length (x_{min}) greater than which the power law function is valid, was determined using Kolmogorov-Smirnov statistics (Clauset et al., 2009). To ensure good parameter estimates, each fit was bootstrapped (100 replicates), to obtain mean and standard deviation values of both $\widehat{x}_{min}$ and $\widehat{\alpha}$. Calculations were performed in RStudio (version 4.1.2) (R Core Team, 2019) using with the poweRlaw package (Gillespie, 2015).

2.5.2. Carbonyl index of released microplastics

To assess the oxidation status of the released microplastics, we randomly selected 10 to 20 microplastics after UV exposure at treatment levels 57-day and 76-day UV, for each polymer type (for detailed number of particles per treatment see Fig. 5) and calculated their carboxyl index (CI), according to Simon-Sánchez et al. (2022) and Beltrán-Sanahuja et al. (2020). Considering that few microplastics were detected in pristine samples (PP: 1 ± 1 microplastics, Table S1), we manually abraded some particles from extra pristine items from each polymer, prepared these particles the same way as the samples by staining them with Nile red and filtered onto PTFE, and then randomly selected the spectra of 20 PP and 14 PLA microplastics ($\geq$ 50 μm). Prior to calculations, all spectra data were first processed in RStudio (version 4.1.2) (R Core Team, 2019) with the ChemoSpec package (Hanson, 2022) for correcting baselines and normalization. The CI value for each PP spectrum was then calculated as the ratio between the integrated band absorbance of the carbonyl (C═O) peak from 1850 to 1650 cm^{-1} and that of the methylene (CH_2) scissoring peak from 1500 to 1420 cm^{-1} (Almond et al., 2020). For PLA, the value was calculated as the ratio between the integrated band absorbance of the carbonyl (C═O) peak from 1850 to 1600 cm^{-1} and that of the carbon-oxygen (C-O) peak from 1340 to 950 cm^{-1} (Beltrán-Sanahuja et al., 2020). For both PLA and PP, an increase of CI value indicates the occurrence of photo-oxidation (Beltrán-Sanahuja et al., 2020; Simon-Sánchez et al., 2022).

2.5.3. Statistical analysis

Statistical analysis was performed using RStudio (R version 4.1.2) (R Core Team, 2019). Data concerning the concentrations of released microplastics per surface area of plastic items (microplastics / cm^2) and the width-to-length ratio (W: L) of released microplastics (Niu et al., 2023) were analyzed per polymer using a non-parametric test, because the ANOVA assumptions of normality were not met after data transformation ($p < 0.05$, Shapiro–Wilk test). Therefore, a Kruskal-Wallis rank sum test was performed to check if the concentration and the width-to-length ratio of released microplastics (Niu et al., 2023) was dependent on treatment (UV exposure treatment per polymer, CI 95%). The Dunn's multiple comparison test (p values adjusted with the Bonferroni method) was applied when there were significant differences between treatments, using FSA package (Derek et al., 2023). To compare the concentrations and the width-to-length ratio of released microplastics between PLA and PP (Niu et al., 2023), a Kruskal-Wallis test followed Dunn's multiple comparison test was performed with 57-day and 76-day UV weathered samples. The parameters such as OIT and CI (Niu et al., 2023) were analyzed either with a Kruskal-Wallis rank sum test (if normality was not met) followed by a Dunnett's test using DescTool (Andri et al., 2021) or with a one-way ANOVA test followed by Tukey's HSD to check if these endpoints were dependent on the duration (day) of UV weathering or polymer compositions.

2.6. Quality criteria and quality control

Several Quality Criteria and Quality Control (QA/QC) (de Ruijter et al., 2020) measures were implemented during the experimental procedures to avoid contamination of the samples by airborne fibers and other particles, and cross contamination between samples. All solvents used were of analytical grade with minimal impurities. All glassware was pre-cleaned using diluted decon-90 detergent and rinsed thoroughly with Milli-Q water and acetone. Potential sources of microplastics contamination were minimized by avoiding the use of any plastic equipment and using prewashed glass and metal items. All filtration steps were performed in a clean reversed flow cabinet. Possible mechanical abrasions of tested plastic items and released microplastics by manipulations has been minimized during the UV weathering and microplastics extraction (Fig. 1, no manual damages on the pristine plastic items). Finally, in the rare cases of airborne fiber contamination

(less than 3 fibers per membrane filter), natural fibers were distinguished from sample particles using fluorescence microscopy as stated above (Meyers et al., 2022). Procedural blanks, i.e., observation of filtered 20 mL water samples without plastic items to detect contamination, were carried out throughout the analysis. Our previous work indicates that our procedure (filtration, Nile red staining and microscopic observations) has a recovery rate of 111 ± 17% for PLA particles (50 – 5000 μm) (Le Gall et al., 2022).

3. Results

3.1. Microplastics formation

The release of microplastics, including of both particle- and fiber-shapes-, (50 – 5000 μm, Table S1) was detected in all PLA samples and the majority (22 out of 24) of PP samples. Dark controls had on average 7 ± 4 PLA microplastics and 4 ± 4 PP microplastics. In pristine samples (0 d, Table S1), both PLA and PP samples contained a low number of (PLA: 2 ± 3; PP: 1 ± 1) microplastics. To confirm the polymer compositions of observed microplastics, in total 280 out of 3386 PLA and PP microplastics were analyzed with μ-FTIR. For PLA and PP, a correct match was 86% (48 out of 56 microplastics) and 92% (206 out of 224 microplastics), respectively. For PP items, up to twenty-fold higher concentrations (microplastics / cm^2) of released microplastics were observed after UV radiation compared to the samples kept in dark and in pristine forms (Fig. 2, $p < 0.05$). Extending the UV exposure duration from 57 days to 76 days had no influence ($p = 0.84$) on the concentrations of PP microplastics released (Fig. 2). An exposure of 57 days resulted in: 59 ± 63 microplastics / cm^2 detected, and an exposure of 76 days in 48 ± 26 microplastics / cm^2. The duration of the UV exposure had an effect on the concentration of PLA microplastics observed (Fig. 2). After 76-day incubation, two-fold more microplastics observed in samples exposed to UV (5 ± 2 microplastics / cm^2) than in dark controls (2 ± 1 microplastics / cm^2) (Fig. 2, $p = 0.006$). When comparing the concentrations of microplastics formed at each time step (0, 57 and 76 d), we observed that PP and PLA items had similar concentrations of microplastics at 0 day, but PP items released 10- and 18-fold higher concentration of microplastics than PLA items after 57 and 76 days (Fig. 2, $p < 0.05$).

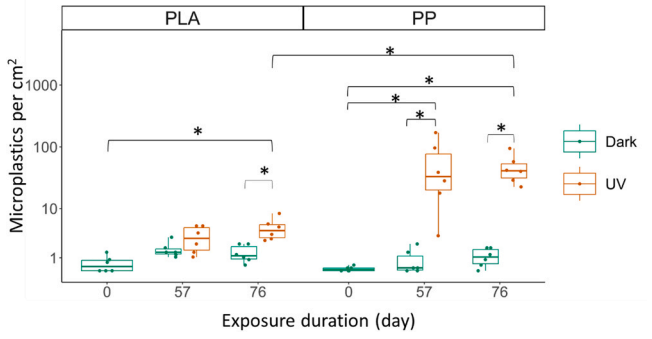

Fig. 2. Boxplots of the release of microplastics from PP and PLA cylinder samples, with median concentrations (microplastics / cm^2) of released microplastics (50 – 5000 μm) versus exposure duration (6 replicates). The concentrations of released microplastics were calculated as the count of microplastics (Table S1) per nominal surface area of plastic items (4.7 cm^2). Y axis were log-transformed with a base of 10. The color of box represents UV exposure (orange) and dark exposure (green). The boxes of pristine samples (0 day) were in green as well. Each dot replicates an individual cylinder. Asterisks (*) indicates statistically significant differences between groups ($p < 0.05$, Dunn's multiple comparison test).

3.2. Size-based characteristics of released microplastics

To obtain size-based characteristics of the microplastics formed and released after exposure to UV radiation and immersion in seawater, cumulative distribution functions for particle length, width and width-to-length-ratio were inferred for all released microplastics after 57-day and 76-day UV exposure (Fig. S2). Particle's length (μm) has a lower limit of 50 μm since we only selected microplastics with a maximum Feret's diameter ≥ 50 μm and an upper limit below 1200 μm, as microplastics larger than 1200 μm exceeded the scale of fluorescent images. Both particles' length and width had discrete steps, which is the result of the pixel-based image analysis.

Power law distributions were fitted on the particles' length for both released PLA and PP microplastics after UV exposure (Fig. 3 and Fig. S2). Mean power law exponents (-) for particles' length were 2.59 ± 0.32 for "57-day UV exposure" PLA samples and 2.38 ± 0.16 for "76-day UV exposure". For PP, the exponents were 2.54 ± 0.06 and 3.04 ± 0.11 (-), respectively (Fig. 3). The minimum particles' length above which the power law distributions valid was 76 ± 26 μm for "57-day UV exposure" PLA samples and 62 ± 20 μm for "76-day UV exposure". For PP, the minimum particle lengths were 65 ± 14 and 103 ± 20 μm, respectively. Below this minimum length, the observations start to deviate from the fitted distribution (Fig. 3).

The duration of UV weathering and the polymer composition had an effect on the width-to-length ratio of released microplastics (Fig. 4). For PLA, no deviation in width-to-length ratio was observed between 57-day and 76-day UV weathered samples ($p = 0.30$). The average width-to-length ratio (-) was 0.54 ± 0.17 in 57-day UV weathered PLA samples, and 0.51 ± 0.17 in 76-day UV weathered PLA samples. For PP, the ratio in samples subject to 76-day UV exposure was higher than 57-day UV weathered samples [57-day: 0.51 ± 0.18 (-), 76-day: 0.57 ± 0.17 (-), $p < 0.001$]. The 76-day UV weathered PP also had a higher width-to-length ratio than 76-day UV weathered PLA samples ($p < 0.01$). Concerning the shape category, 14% and 16% of released PLA microplastics are in fiber-shape in 57-day and 76-day UV exposure samples. For released PP microplastics, the fractions of fiber-shaped microplastics are 18% and 11%, respectively.

3.3. Oxidation status of released microplastics and parent plastic items

The carbonyl index (CI), here used as a metric for oxidation status, of released PP microplastics was altered after exposure to UV weathering (Fig. 5). The mean CI (-) in pristine (0-day), 57-day and 76-day UV weathered samples are 0.73 ± 0.05, 0.70 ± 0.12, and 0.83 ± 0.11, respectively. The CI of microplastics in 76-day UV weathered samples were higher than 57-day UV weathered ($p = 0.02$) and pristine PP microplastics ($p < 0.001$). For PLA, no differences ($p > 0.05$) in CI have been observed as the values of the CI between pristine [1.09 ± 1.13 (-)], 57-day [0.62 ± 0.64 (-)], and 76-day UV-weathered samples [0.52 ± 0.42 (-)].

The SEM images of UV exposed (57-day and 76-day) samples (Fig. 1) indicate fissures and cracks on the surface of parent PP items, a sign of surface degradation, while these features were not observed in PLA samples. The 76-day UV exposed PLA samples had, however, visible micro sized material attached to the surface.

The oxidation induction time (OIT, minutes), which is a measure of oxidation resistance (McKeen, 2014) of both PLA and PP items altered after exposure to UV weathering compared to pristine items (Fig. 6, 3 replicates). For PLA, the mean OIT (minutes) of pristine (0 day), 57-day and 76-day UV weathered items were 2.19 ± 0.10, 2.34 ± 0.04, and 0.16 ± 0.04 min, respectively (3 replicates). The OIT values of 76-day UV weathered PLA items were 13-fold lower than pristine PLA items ($p < 0.001$). For PP, OIT value of both 57-day and 76-day UV weathered items was at least 27-fold lower than the pristine items (pristine: 5.28 ± 0.65 min, 57-day: 0 ± 0 min, 76-day: 0.19 ± 0.02 min, $p < 0.05$).

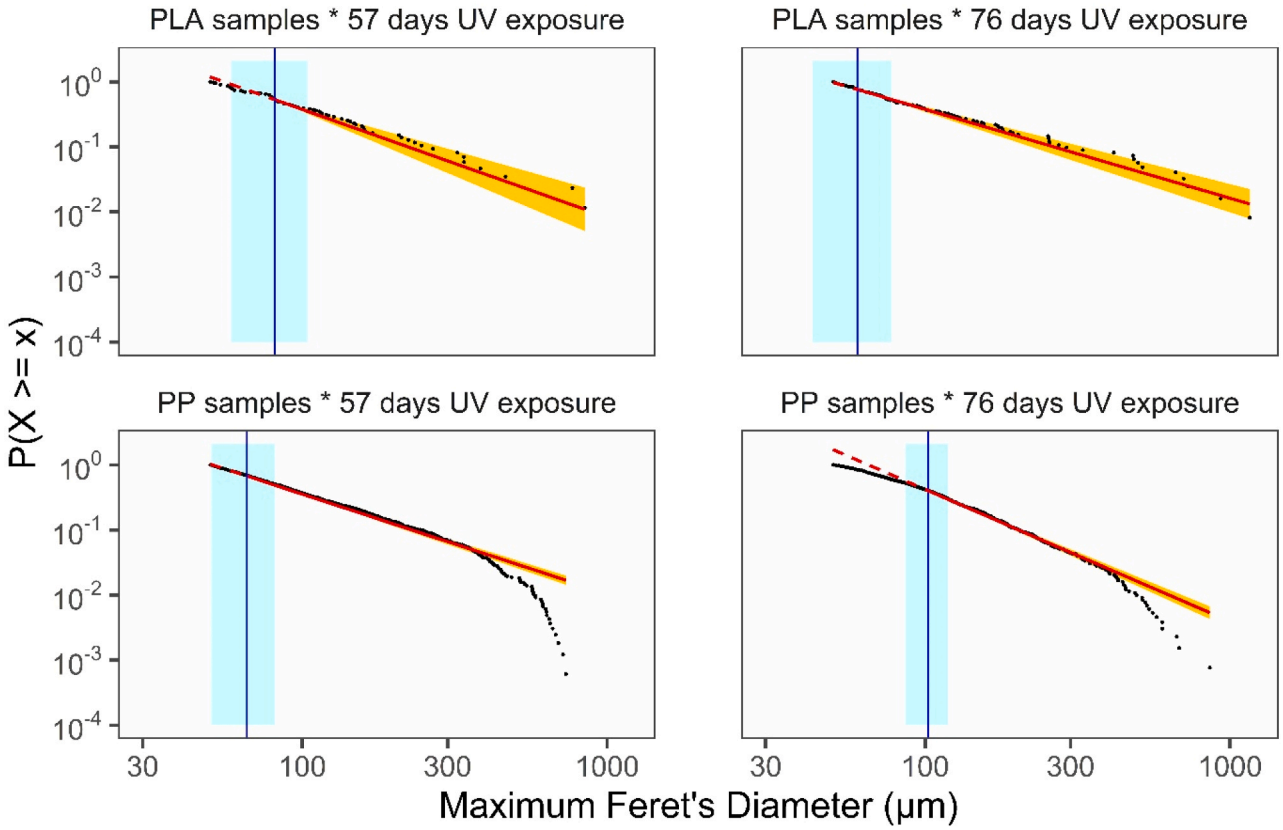

Fig. 3. Particles' length distributions of released microplastics (50 - 1200 μm) from UV-weathered plastic items for both PP and PLA. In the present study, the maximum Feret's diameter (μm) were used as a proxy for particle length. The blue vertical segments indicate the minimum length for which the fitted power law is valid. The red slopes present the fitted power law distributions. The mean (solid line, in red) and standard deviation (shaded area, in yellow) are based on bootstraps with 100 replicates. The dotted line shows the continuation of the fitted slope beyond the minimum size. The minimum particles' lengths (mean ± standard deviation) are 76 ± 26 μm for "57-day UV exposure" PLA samples and 62 ± 20 μm for "76-day UV exposure". For PP, the minimum particle lengths are 65 ± 14 and 103 ± 20 μm, respectively. Mean exponent parameters (mean ± standard deviation) are 2.59 ± 0.32 and 2.38 ± 0.16 (-) for PLA samples subjected to 57 and 76-day UV irradiance. For PP samples, these are 2.54 ± 0.06 and 3.04 ± 0.11 (-), respectively.

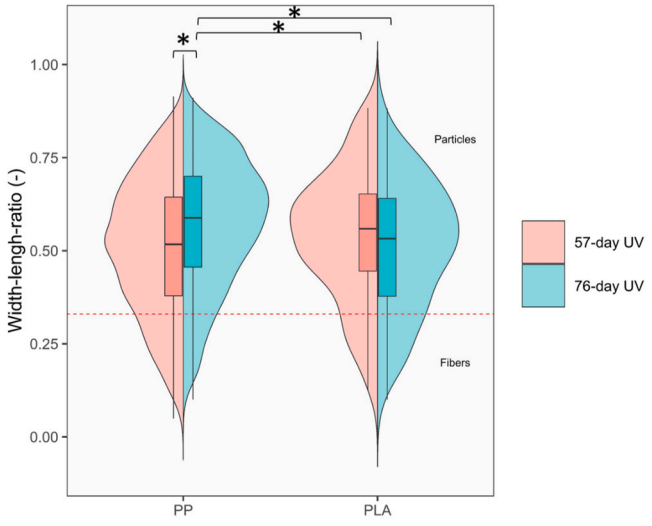

Fig. 4. Violin- and box-plot of the aspect ratio of released microplastics from both PLA and PP after UV radiation. Color of box represents samples subject to 57-day (pink) and 76-day (blue) UV radiation, respectively. The horizontal intercept line (red and dashed) represents the aspect ratio of 0.33, above which the released microplastics were considered as "particles", then the rest were "fibers". Asterisks (*) indicates statistically significant differences between groups ($p < 0.05$, Dunn's multiple comparison test).

4. Discussion

4.1. Microplastics formation

A 76-day UV radiation exposure of polypropylene (PP) and polylactic acid (PLA) items immersed in seawater accelerated the released of microplastics, with PLA items being more resistant to fragmentation and to releasing microplastics than PP items (Fig. 2). We observed that up to nine-fold higher concentrations of released microplastics were detected in PP samples (48 ± 26 microplastics / cm^2) than from PLA samples (5 ± 2 microplastics / cm^2) after 76-day UV exposure (Fig. 2, $p < 0.05$), suggesting that the tested PLA items are less prone to fragmentation and releases of microplastics (50 – 5000 μm) than PP items. The mean concentration of released PLA microplastics in the present study were within the same magnitude as our previous work (Le Gall et al., 2022) where 2.2 microplastics / cm^2 (50 – 5000 μm) were detected in 38-day UV weathered PLA samples. The accelerated release of microplastics after similar duration of UV radiation was confirmed by Lambert and Wagner (2016) and Song et al. (2022), however, the abundance of released microplastics per surface area of parent plastic items, reported in these studies were orders of magnitude higher than the present work (Table 1). For example, in the work of Song et al. (2022), 67,000 PP microplastics / cm^2 (0.8 – 500 μm) were detected in sample subjected to a 60-day (i.e., equivalent to 53-day of the present study, Table 1) UV radiation. Although the environmental matrix used in these studies [i.e. deionized water in Lambert and Wagner (2016)] are different from the present study (filtered natural seawater, section2.1), however, neither

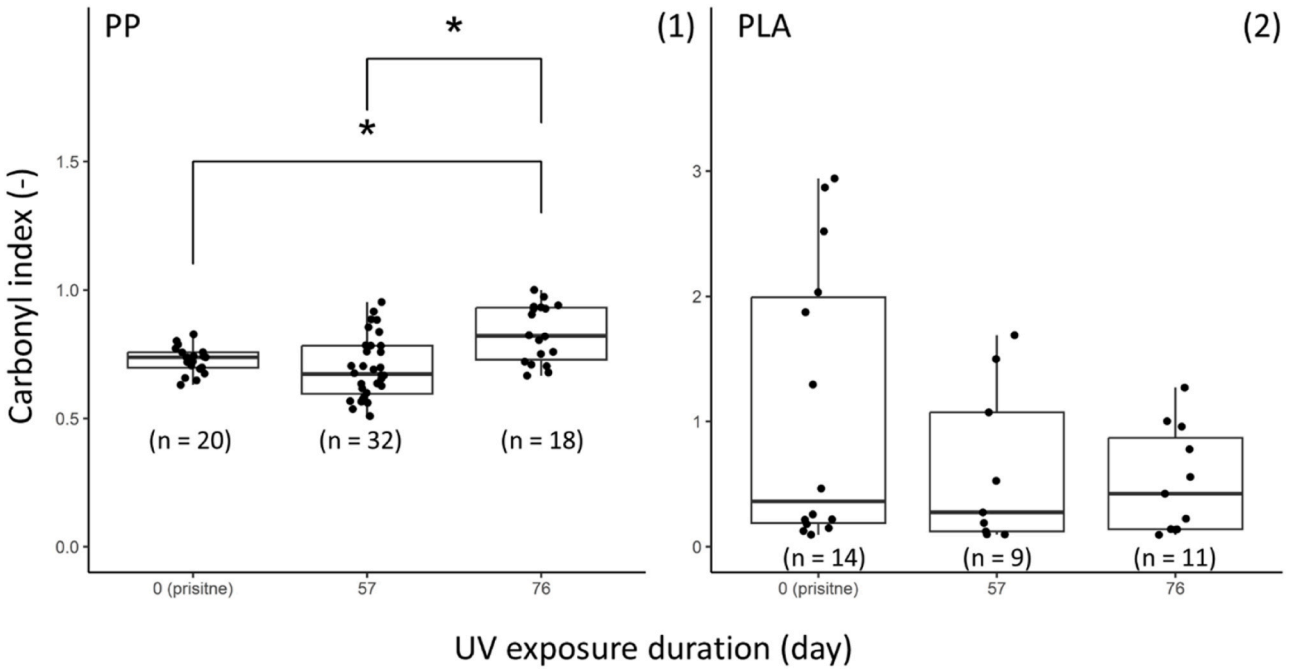

Fig. 5. Boxplot of carbonyl index (CI) of randomly selected PP microplastics, with median CI value versus exposure duration. Number of spectra per treatment were labeled next to the corresponding boxes. Asterisks (*) indicates statistically significant differences between groups ($p < 0.05$, Tukey's HSD).

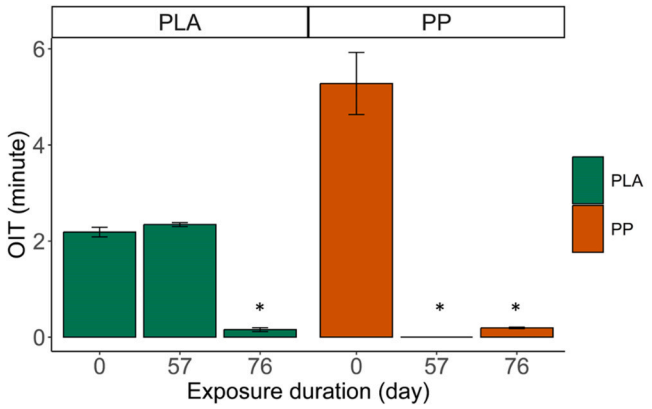

Fig. 6. Bar chart of mean oxidation induction time (OIT, minute) from PP and PLA cylinder samples, with corresponding standard deviation of retrieved items versus UV weathering duration (3 replicates). The color represents PP (orange) and PLA (green). Error bars represent the standard deviation. Asterisks (*) shows statistically significant differences with pristine items (0 day) per polymer ($p < 0.05$, Dunnett's test).

the present work (Fig. 2) nor above-mentioned studies have observed an effect of environmental matrix, as per Wei et al. (2021). Thus, we identified a potential reason for the order of magnitude difference as the varied target size range of released microplastics, coupled with the corresponding microplastics quantification techniques, among studies. As observed in the present study (Fig. 3), and others (Song et al., 2017; Kaandorp et al., 2021), the abundance of released microplastics, as a result of particle fragmentation, follows a power law curve with negative exponent against particle size, suggesting that the observed abundance of released microplastics would be orders of magnitude higher if smaller sized microplastics was included (see section 4.2 for further discussion). Therefore, to enhance the comparability of plastic fragmentation in future research, it is recommended that abundance data among different microplastic quantification techniques be standardized. A possible method to achieve this standardization is by employing particle size distribution analysis (Koelmans et al., 2020). Also, the standard deviation of microplastics concentration in the present work was large, especially in UV weathered PP samples (57-day: relative standard deviation = 107%), but this can be attributed to the nature of particle fragmentation and is often observed in microplastics formation studies [e.g. 176% in Song et al. (2022)].

The initiation of fragmentation from the tested PP items was also

Table 1
Summary of microplastic formation results of PLA and PP under UV radiation among studies.

Reference	polymer type	Surface area of parent plastics (cm^2)	UV duration (day)	Total UV irradiance (MJ / m^2)	Size range (μm)	Concentration (particles / cm^3)
Le Gall et al. (2022)	SR-PLA	17.8	38 (38[a])	197	50 - 5000	2.2
Present study	PLA	4.7	57	295	50 - 5000	3.2
			76	394		4.7
	PP		57	295		59.1
			76	394		47.7
Song et al. (2022)	PP	37.2	60 (53[a])	275	0.8 - 500	67,000
			120 (106[a])	550		150,000
			180 (160[a])	829		210,000
Lambert and Wagner (2016)	PLA	2.8	84	-[b]	2 - 60	142,857
	PP	2.12				3773,585

[a] UV duration (day) normalized to conditions of the present study.
[b] Could not be calculated as a lack of necessary information.

faster than from PLA items (Fig. 2). Up to 44-fold higher concentrations of released PP microplastics were found in samples subjected to 57-day UV radiation than in samples kept in dark for the same duration (Fig. 2, e.g. 57-day UV: 59 ± 57 PP microplastics / cm^2, 57-day dark: 1 ± 1 PP microplastics / cm^2), suggesting that 18 months of mean solar radiation in Europe (Gewert et al., 2018) initialized the fragmentation and accelerated the release of microplastics for PP items. For PLA, this was observed only after 76-day UV radiation (Fig. 2), equivalent to 24 months of mean solar radiation in Europe (Gewert et al., 2018). The SEM inspection of recovered plastics items (Fig. 1) confirmed that the presence of cracks formed on the surface of PP items after 57-day and 76-day UV radiation, indicating the occurrence of photo-degradation induced by UV and the subsequent fragmentation, but the same was not observed in PLA items. Although we did not observe an increase in the concentration of released PP microplastics by extending the UV exposure duration from 57 to 76 days (Fig. 2), our size frequency distribution estimates (Fig. 3) indicated that there were more PP microplastics that were smaller than 50 μm (see section 4.2 for further discussion), and which were not within our range of enumeration. In the present study, it should be noted that 76-day UV weathered PLA items had various micro-particles attached onto their surface (Fig. 1), which were not quantified in the present work, but indicate that microplastics formation patterns are ongoing and particles could have been detached after a prolonged exposure (Song et al., 2022).

In accordance with the observed microplastics releasing patterns (Fig. 2), pristine PLA items showed a better resistance to oxidation induced by UV than pristine PP items (Fig. 6). The OIT of PP items decreased to 0 ± 0 min, after 57-day UV exposure (Fig. 6), suggesting that PP items lost almost all oxidative resistance (McKeen, 2014). For PLA, the loss of oxidative resistance was only observed after 76-day exposure with an OIT value of 0.16 ± 0.04 min. This is in line with the order of their bond dissociation energy under UV irradiation where PP (77 kcal / mol) < polyester (88 kcal / mol), i.e. a polymer similar as PLA in chemical structure (Feldman, 2002). The FTIR spectra of released microplastics (Fig. S3) confirmed that in carbonyl products (1710 cm^{-1}), the characteristic peak of the photo-oxidation of PP (Wu et al., 2021), observed in 57-day and 76-day UV weathered PP samples, while no formation of anhydride groups (1845 cm^{-1}) (Gardette et al., 2011) were observed even in 76-day UV weathered PLA samples. In the present study, there is a slight increase (0.15 min) in the mean OIT value of 57 PLA items exposed to 57-day UV radiation compared to pristine items and a slight decrease (0.19 min) in PP items by extending the UV exposure from 57 to 76 days. These changes are within the heterogeneity between plastic items tested in the present work, demonstrated by the mean OIT of pristine PLA (2.19 ± 0.10 min) and PP (5.28 ± 0.65 min) items.

In addition to polymer composition, the presence of potential plastic additives in the matrix can partly contribute to the observed differences. For example, UV stabilizers can protect plastics from photo-oxidation induced by UV (Curto et al., 2021), which may alter their resistance to photo-oxidation and thus microplastics formation (Sørensen et al., 2021). A recent study reported that stabilizers prevented the photo-degradation and microplastics formation of PP samples for 14.5 day under UV exposure (same irradiation intensity as the present study) and deionized water immersion (Meides et al., 2022). Nevertheless, plastic additives in the materials used in our study were not documented. In future research on microplastic formation, it is recommended to analyze and provide information on the additives present in the tested plastics, if feasible (Sørensen et al., 2021), and to further explore to which extent plastic additives can affect the plastic fragmentation and release of microplastics of different polymers, especially of bio-based polymers.

PLA items tested in the present study released two times more microplastics after a 76-day UV radiation compared to dark control samples (Fig. 2), suggesting that bio-based plastics can act as a potential source of microplastics in the marine environment. Currently, bio-based plastics are promoted as alternative to petroleum-based plastics, however, to better assess their environmental risk, i.e. Koelmans et al. (2022), the quantification and characterization of releasing microplastics to the environment is required. Although not observed in the present study (i.e. a sterile environment), Bao et al. (2022) reported that poly (butyleneadipate-co-terephthalate), a bio-based and biodegradable plastic, can be fragmented by microorganisms and release up to fourteen times more microplastics than polyvinyl chloride. Therefore, although bio-based plastics may have a slower release of fragmented particles under UV radiation compared to conventional polymer types, their potential to release microplastics to the environment need to be considered to avoid unintentional adverse effects in biota.

4.2. Characterization of released microplastics

The size and shape distribution of released microplastics (50 – 1200 μm) after UV radiation was different between polymers (Fig. 3 and Fig. 4). The power law exponent of particles' length distributions of released microplastics (α), for 76-day UV weathered PLA was smaller [2.38 ± 0.16 (-), Fig. 3] than the value of 76-day UV weathered PP [3.04 ± 0.11 (-), Fig. 3]. These results suggest that the released PLA microplastics have a larger-sized fraction than PP microplastics And that the difference in α between PLA and PP can be attributed to the degree of fragmentation (Kaandorp et al., 2021). For example, the α of 76-day UV weathered PP samples exceeds a theoretically threshold of cascading fragmentation[α = 3 (-)] at all three-dimensions (Kaandorp et al., 2021), indicating that the released PP microplastics were also being broken down to smaller sized microplastics along their longest dimension (Kaandorp et al., 2021). In this case, despite similar microplastics (50 – 5000 μm) concentrations being detected in 57-day and 76-day of UV weathered PP samples, we estimated that a higher microplastics concentration is in fact present in 76-day UV-weathered PP samples, but these particles were below the threshold for the size fraction assessed (i.e. 50 μm). The shape distribution of released PP microplastics can also be explained by the cascading fragmentation. For the PP particles, the width-to-length ratio (W: L) increased and the fiber-shaped microplastics fractions deceased when the UV exposure duration was extended from 57 to 76 days (Fig. 4), resulting most likely from the break-down of PP microplastics along their longest dimension. With respect to PLA samples, the α for both 57 and 76-day UV weathered PLA were lower than the threshold of cascading fragmentation in two-dimensions. Therefore, the difference in microplastics concentrations (Fig. 2) and shape distributions (Fig. 4) were expected as new PLA microplastics were still directly being released from the parent plastic items in 76-day UV weathered samples.

The size and shape of released microplastics up to 76-day UV radiation were similar to microplastics retrieved from aquatic environments. The fitted α released PP microplastics in the present study were within the reported exponent ranges for PP microplastics retrieved from general aquatic environment [mean alpha = 2.70 (-)(Kooi et al., 2021)]. For PLA, the fitted exponent was within the range of environmental polyester [mean alpha ≈ 2.6 (-), (Kooi et al., 2021)]. The comparable patterns are confirmed when comparing their average width-to-length ratio and fiber-shaped microplastics fractions with microplastics in aquatic environment (Kooi et al., 2021). This finding suggests that microplastics in aquatic environments are still at initial stage of fragmentation (Koelmans et al., 2022), although a study in 2015 calculated that 90% of plastics in the oceans have been present for more than 2 years (Koelmans et al., 2016) (the equivalent solar irradiation exposure in the present study). In this case, even under the system change scenario [reduced plastic pollution by 40% from 2016 rates (Lau et al., 2020)], an increased microplastics concentration in the aquatic environment can be expected from fragmentation of the "legacy" plastics in a near future (Okamoto, 2020).

The size and shape distribution of released microplastics (50 – 1200 μm) determined in the present study is valuable in a future

environmental risk assessment of bio- and petroleum-based microplastics. For example, based on the power law exponent α observed in our study, concentrations of bio-based microplastics can be rescaled into the (bio)accessible fractions for different aquatic species via ingestion, to support further realistic ecotoxicological effect assessments as per the work of Koelmans et al. (2020). Specifically, the quantified PLA and PP particles length (50 – 1200 μm) can be relevant for the microplastics mis-ingestion of zooplankton and fish (Jâms et al., 2020). The determined particles' shape distribution is considered relevant for shape-specific toxicity, as for example fiber-shaped microplastics (PP, in our study), with a longer retention time in gut, can induce more harmful effects than particle-shaped microplastics (de Ruijter et al., 2020).

Both PLA and PP, microplastics released after 76-day UV exposure were still pristine (Fig. 5), in what concerns their oxidation status. The mean carbonyl index (CI) of released PLA microplastics in 57-day and 76-day UV weathered samples was not different from pristine PLA microplastics (Fig. 5, $p > 0.05$). This is consistent with no formation of anhydride groups (1845 cm^{-1}), the characteristic groups of PLA photo-oxidation (Gardette et al., 2011), was observed even in 76-day UV weathered PLA (Fig. S3). As the OIT results indicate (Fig. 6), PLA items only lost oxidation resistance after 76-day UV radiation (Fig. 6), which indicates that the mean CI value of released PLA microplastics might increase only after prolonged UV exposure (Beltrán-Sanahuja et al., 2020). For PP microplastics, the mean CI value increased by 14% after a 76-day UV exposure (Fig. 5), suggesting the increasing contents of carbonyl products (1710 cm^{-1}) (Wu et al., 2021). Despite an increase of mean CI value (Fig. 5), the released PP microplastics (the present study) are still pristine compared to microplastics in the aquatic environment. For example, CI of PP microplastics 76-day UV weathered samples (Fig. 5) is 50% less than PP microplastics extracted from the surface (depth = 0.5 cm) of marine sediments (Simon-Sánchez et al., 2022). Therefore, a longer UV exposure duration (d) UV or a higher radiation intensity (W / m^2) is required for those seeking a relationship between UV dose and CI of microplastics released by fragmentation (Song et al., 2022).

5. Conclusion

In the present study, we quantified and characterized the fragmentation and release of microplastics from a bio- and a petroleum-based plastic after exposure to UV radiation and seawater immersion. The tested bio-based polymer PLA was more resistant to fragmentation than the petroleum-based polymer PP (24 months mean solar radiation in Europe). The PLA items released nine-times less microplastics than PP items, implying a lower fragmentation rate for the types of plastic tested. The size and shape distribution of released microplastics (50 – 1200 μm) was polymer-dependent. The released PP microplastics had higher smaller-sized and lower fiber-shaped fractions than PLA microplastics. Even though replacing petroleum-based plastics by bio-based alternatives is set forward as being part of a set of potential solutions for the plastic pollution issue in the marine environment, regulators should consider the durability of materials and the potential to release microplastics to avoid unintentional adverse effects in biota.

Funding

The SeaBioComp project has received funding from the Interreg 2 Seas programme 2014–2020 cofounded by the European Regional Development Fund under subsidy contract number 2506–006. Zhiyue Niu was further supported by the Flanders Innovation & Entrepreneurship (VLAIO) in the capacity of the PLUXIN project 'Plastic Flux for Innovation and Business Opportunities in Flanders' (cSBO, Project Number HBC.2019.2904).

CRediT authorship contribution statement

Zhiyue Niu: Conceptualization, Formal analysis, Investigation, Methodology, Visualization, Writing – original draft. **Marco Curto:** Formal analysis, Investigation, Methodology, Writing – review & editing. **Maelenn Le Gall:** Formal analysis, Investigation, Methodology, Writing – review & editing. **Elke Demeyer:** Funding acquisition, Methodology, Writing – review & editing. **Jana Asselman:** Supervision, Writing – review & editing. **Colin R Janssen:** Supervision, Writing – review & editing. **Hom Nath Dhakal:** Funding acquisition, Methodology, Supervision, Writing – review & editing. **Peter Davies:** Funding acquisition, Methodology, Writing – review & editing. **Ana Isabel Catarino:** Conceptualization, Methodology, Supervision, Writing – review & editing. **Gert Everaert:** Conceptualization, Funding acquisition, Methodology, Supervision, Writing – review & editing.

Declaration of Competing Interest

The authors declare the following financial interests/personal relationships which may be considered as potential competing interests: The authors Elke Demeyer is employed by Centexbel (Ghent, BE), a private company highly active in the knowledge transfer of textile and plastic processing industry. The other authors report no conflict of interest.

Data availability

The dataset produced and presented in the work are openly available in the online repository Marine Data Archive, https://doi.org/10.14284/640.

Acknowledgments

The authors thank the LifeWatch Observatory as part of the Flemish contribution to the LifeWatch ESFRI by Flanders Marine Institute, Belgium, for use of their binocular microscope. The authors would also like to thank Mr. Mattias Bossaer and Ms. Julie Muyle (Technical Assistant Research, Flanders Marine Institute, Belgium) for their assistance on laboratory work.

Appendix A. Supporting information

Supplementary data associated with this article can be found in the online version at doi:10.1016/j.ecoenv.2024.115981.

References

Alexy, P., Anklam, E., Emans, T., Furfari, A., Galgani, F., Hanke, G., et al., 2020. Managing the analytical challenges related to micro- and nanoplastics in the environment and food: filling the knowledge gaps. Food Addit. Contam. - Part A Chem. Anal. Control. Expo. Risk Assess. 37, 1–10. https://doi.org/10.1080/19440049.2019.1673905.

Almond, J., Sugumaar, P., Wenzel, M.N., Hill, G., Wallis, C., 2020. Determination of the carbonyl index of polyethylene and polypropylene using specified area under band methodology with ATR-FTIR spectroscopy. E-Polym. 20, 369–381. https://doi.org/10.1515/epoly-2020-0041.

Andri, S., Ken, A., Andreas, A., Nanina, A., Tomas, A., Chandima, A., Antti, A., Adrian, B., Kamil, B., Ben, B., 2021. DescTools: Tools for descriptive statistics. R Packag. version 0.99 43.

Au, S.Y., Bruce, T.F., Bridges, W.C., Klaine, S.J., 2015. Responses of Hyalella azteca to acute and chronic microplastic exposures. Environ. Toxicol. Chem. 34, 2564–2572. https://doi.org/10.1002/etc.3093.

Bao, R., Cheng, Z., Hou, Y., Xie, C., Pu, J., Peng, L., et al., 2022. Secondary microplastics formation and colonized microorganisms on the surface of conventional and degradable plastic granules during long-term UV aging in various environmental media. J. Hazard. Mater. 439, 129686 https://doi.org/10.1016/j.jhazmat.2022.129686.

Beltrán-Sanahuja, A., Casado-Coy, N., Simó-Cabrera, L., Sanz-Lázaro, C., 2020. Monitoring polymer degradation under different conditions in the marine environment. Environ. Pollut. 259, 113836 https://doi.org/10.1016/j.envpol.2019.113836.

Clauset, A., Shalizi, C.R., Newman, M.E.J., 2009. Power-law distributions in empirical data. SIAM Rev. 51, 661–703. https://doi.org/10.1137/070710111.
R. Core Team (2019). R: A language and environment for statistical computing. *R Found. Stat. Comput. Vienna, Austria.* Available at: ⟨https://www.r-project.org/⟩.
Cózar, A., Echevarría, F., González-Gordillo, J.I., Irigoien, X., Úbeda, B., Hernández-León, S., et al., 2014. Plastic debris in the open ocean. Proc. Natl. Acad. Sci. U. S. A 111, 10239–10244. https://doi.org/10.1073/pnas.1314705111.
Curto, M., Le Gall, M., Catarino, A.I., Niu, Z., Davies, P., Everaert, G., et al., 2021. Long-term durability and ecotoxicity of biocomposites in marine environments: a review. RSC Adv. 11, 32917–32941. https://doi.org/10.1039/d1ra03023j.
de Ruijter, Redondo-Hasselerharm, V.N., Gouin, P.E., Koelmans, T., Ruijter, A.A., De, V. N., Redondo-Hasselerharm, P.E., et al., 2020. Quality Criteria for Microplastic Effect Studies in the Context of Risk Assessment: A Critical Review. Environ. Sci. Technol. 54, 11692–11705. https://doi.org/10.1021/acs.est.0c03057.
Derek, H.O., Jason, C.D., Wheeler, A.P., and Dinno, A. (2023). FSA: Simple Fisheries Stock Assessment Methods. Available at: ⟨https://cran.r-project.org/package=FSA⟩.
European Bioplastics (2021). Bioplastics market development update 2021.
Everaert, G., Vlaeminck, K., Vandegehuchte, M.B., Janssen, C.R., 2022. Effects of microplastic on the population dynamics of a marine copepod: insights from a laboratory experiment and a mechanistic model. Environ. Toxicol. Chem. 0 https://doi.org/10.1002/etc.5336.
Feldman, D., 2002. Polymer weathering: Photo-oxidation. J. Polym. Environ. 10, 163–173. https://doi.org/10.1023/A:1021148205366.
Gardette, M., Thérias, S., Gardette, J.-L., Murariu, M., Dubois, P., 2011. Photooxidation of polylactide/calcium sulphate composites. Polym. Degrad. Stab. 96, 616–623. https://doi.org/10.1016/j.polymdegradstab.2010.12.023.
Gewert, B., Plassmann, M.M., Macleod, M., 2015. Pathways for degradation of plastic polymers floating in the marine environment. Environ. Sci. Process. Impacts 17, 1513–1521. https://doi.org/10.1039/c5em00207a.
Gewert, B., Plassmann, M., Sandblom, O., Macleod, M., 2018. Identification of Chain Scission Products Released to Water by Plastic Exposed to Ultraviolet Light. Environ. Sci. Technol. Lett. 5, 272–276. https://doi.org/10.1021/acs.estlett.8b00119.
Gillespie, C.S., 2015. Fitting Heavy Tailed Distributions: The poweRlaw Package. J. Stat. Softw. 64, 1–16. https://doi.org/10.18637/jss.v064.i02.
Hanson, B.A. (2022). ChemoSpec: Exploratory Chemometrics for Spectroscopy. Available at: ⟨https://cran.r-project.org/package=ChemoSpec⟩.
Hartmann, N.B., Hüffer, T., Thompson, R.C., Hassellöv, M., Verschoor, A., Daugaard, A. E., et al., 2019. Are We Speaking the Same Language? Recommendations for a Definition and Categorization Framework for Plastic Debris. Environ. Sci. Technol. 53, 1039–1047. https://doi.org/10.1021/acs.est.8b05297.
ISO, 2006, 4892-2 Plastics–Methods of exposure to laboratory light sources–Part 2: xenon-arc sources.
ISO, 2018, 11357–6 Plastics—Differential Scanning Calorimetry (DSC)—Part 6. Determination of Oxidation Induction Time (Isothermal OIT) and Oxidation Induction Temperature (Dynamic OIT).
Jâms, I.B., Windsor, F.M., Poudevigne-Durance, T., Ormerod, S.J., Durance, I., 2020. Estimating the size distribution of plastics ingested by animals. Nat. Commun. 11 (1), 7. https://doi.org/10.1038/s41467-020-15406-6.
Kaandorp, M.L.A., Dijkstra, H.A., van Sebille, E., 2021. Modelling size distributions of marine plastics under the influence of continuous cascading fragmentation. Environ. Res. Lett. 16 https://doi.org/10.1088/1748-9326/abe9ea.
Koelmans, A.A., Bakir, A., Burton, G.A., Janssen, C.R., 2016. Microplastic as a Vector for Chemicals in the Aquatic Environment: Critical Review and Model-Supported Reinterpretation of Empirical Studies. Environ. Sci. Technol. 50, 3315–3326. https://doi.org/10.1021/acs.est.5b06069.
Koelmans, A.A., Redondo-Hasselerharm, P.E., Mohamed Nor, N.H., Kooi, M., 2020. Solving the nonalignment of methods and approaches used in microplastic research to consistently characterize risk. Environ. Sci. Technol. 54, 12307–12315. https://doi.org/10.1021/acs.est.0c02982.
Koelmans, A.A., Redondo-Hasselerharm, P.E., Nor, N.H.M., de Ruijter, V.N., Mintenig, S. M., Kooi, M., 2022. Risk assessment of microplastic particles. Nat. Rev. Mater. 7, 138–152. https://doi.org/10.1038/s41578-021-00411-y.
Kooi, M., Primpke, S., Mintenig, S.M., Lorenz, C., Gerdts, G., Koelmans, A.A., 2021. Characterizing the multidimensionality of microplastics across environmental compartments. Water Res 202, 117429. https://doi.org/10.1016/j.watres.2021.117429.
Lambert, S., Wagner, M., 2016. Formation of microscopic particles during the degradation of different polymers. Chemosphere 161, 510–517. https://doi.org/10.1016/j.chemosphere.2016.07.042.
Lau, W.W.Y.Y., Shiran, Y., Bailey, R.M., Cook, E., Stuchtey, M.R., Koskella, J., et al., 2020. Evaluating scenarios toward zero plastic pollution. Science 369 (80), 1455–1461. https://doi.org/10.1126/SCIENCE.ABA9475.
Le Gall, M., Niu, Z., Curto, M., Catarino, A.I., Demeyer, E., Jiang, C., et al., 2022. Behaviour of a self-reinforced polylactic acid (SRPLA) in seawater. Polym. Test. 111, 107619 https://doi.org/10.1016/j.polymertesting.2022.107619.
McDowell, G.R., Bolton, M.D., 1998. On the micromechanics of crushable aggregates. Geotechnique 48, 667–679. https://doi.org/10.1680/geot.1998.48.5.667.
McKeen, L.W., 2014. Introduction to the effect of heat aging on plastics. Eff. Long. Term. Therm. Expo. Plast. Elastomers 17–42. https://doi.org/10.1016/b978-0-323-22108-5.00002-3.
Meides, N., Mauel, A., Menzel, T., Altstädt, V., Ruckdäschel, H., Senker, J., et al., 2022. Quantifying the fragmentation of polypropylene upon exposure to accelerated weathering. Micro Nanoplastics 2. https://doi.org/10.1186/s43591-022-00042-2.
Meyers, N., Catarino, A.I., Declercq, A.M., Brenan, A., Devriese, L., Vandegehuchte, M., et al., 2022. Microplastic detection and identification by Nile red staining: Towards a semi-automated, cost- and time-effective technique. Sci. Total Environ. 823, 153441 https://doi.org/10.1016/j.scitotenv.2022.153441.
Niu, Z., Curto, M., Le Gall, M., Demeyer, E., Asselman, J., Janssen, C.R., et al., 2023. Microplastics formation data on polylactic acid and polypropylene items after UV radiation and seawater immersion. Mar. Data Arch. https://doi.org/10.14284/640.
Okamoto, S., 2020. Flipping handedness in ferrimagnets. Nat. Mater. 19, 929–930. https://doi.org/10.1038/s41563-020-0779-4.
Okoffo, E.D., Chan, C.M., Rauert, C., Kaserzon, S., Thomas, K.V., 2022. Identification and Quantification of Micro-Bioplastics in Environmental Samples by Pyrolysis-Gas Chromatography-Mass Spectrometry. Environ. Sci. Technol. 56, 13774–13785. https://doi.org/10.1021/acs.est.2c04091.
Sandler, N., Wilson, D., 2010. Prediction of granule packing and flow behavior based on particle size and shape analysis. J. Pharm. Sci. 99, 958–968. https://doi.org/10.1002/jps.21884.
SAPEA, 2019. A Scientific Perspective on Microplastics in Nature and Society. Berlin. https://doi.org/10.26356/microplastics.
SAPEA *Biodegradability of Plastics in the Open Environment* 2020 doi: 10.26356/biodegradabilityplastics.
Schindelin, J., Arganda-Carreras, I., Frise, E., Kaynig, V., Longair, M., Pietzsch, T., et al., 2012. Fiji: an open-source platform for biological-image analysis. Nat. Methods 9, 676–682. https://doi.org/10.1038/nmeth.2019.
Simon, M., van Alst, N., Vollertsen, J., 2018. Quantification of microplastic mass and removal rates at wastewater treatment plants applying Focal Plane Array (FPA)-based Fourier Transform Infrared (FT-IR) imaging. Water Res 142, 1–9. https://doi.org/10.1016/j.watres.2018.05.019.
Simon, M., Vianello, A., Shashoua, Y., Vollertsen, J., 2021. Accelerated weathering affects the chemical and physical properties of marine antifouling paint microplastics and their identification by ATR-FTIR spectroscopy. Chemosphere 274. https://doi.org/10.1016/j.chemosphere.2021.129749.
Simon-Sánchez, L., Grelaud, M., Lorenz, C., Garcia-Orellana, J., Vianello, A., Liu, F., et al., 2022. Can a Sediment Core Reveal the Plastic Age? Microplastic Preservation in a Coastal Sedimentary Record. Environ. Sci. Technol. 56, 16780–16788. https://doi.org/10.1021/acs.est.2c04264.
Song, Y.K., Hong, S.H., Eo, S., Shim, W.J., 2022. The fragmentation of nano- and microplastic particles from thermoplastics accelerated by simulated-sunlight-mediated photooxidation. Environ. Pollut. 311, 119847 https://doi.org/10.1016/j.envpol.2022.119847.
Song, Y.K., Hong, S.H., Jang, M., Han, G.M., Jung, S.W., Shim, W.J., 2017. Combined effects of UV exposure duration and mechanical abrasion on microplastic fragmentation by polymer type. Environ. Sci. Technol. 51, 4368–4376. https://doi.org/10.1021/acs.est.6b06155.
Sørensen, L., Groven, A.S., Hovsbakken, I.A., Del Puerto, O., Krause, D.F., Sarno, A., et al., 2021. UV degradation of natural and synthetic microfibers causes fragmentation and release of polymer degradation products and chemical additives. Sci. Total Environ. 755, 143170 https://doi.org/10.1016/j.scitotenv.2020.143170.
Ter Halle, A., Ladirat, L., Gendre, X., Goudouneche, D., Pusineri, C., Routaboul, C., et al., 2016. Understanding the Fragmentation Pattern of Marine Plastic Debris. Environ. Sci. Technol. 50, 5668–5675. https://doi.org/10.1021/acs.est.6b00594.
Wei, X.F., Bohlén, M., Lindblad, C., Hedenqvist, M., Hakonen, A., 2021. Microplastics generated from a biodegradable plastic in freshwater and seawater. Water Res 198, 117123. https://doi.org/10.1016/j.watres.2021.117123.
Wu, H., Zhao, Y., Dong, X., Su, L., Wang, K., Wang, D., 2021. Probing into the microstructural evolution of isotactic polypropylene during photo-oxidation degradation. Polym. Degrad. Stab. 183, 109434 https://doi.org/10.1016/j.polymdegradstab.2020.109434.
Ziajahromi, S., Kumar, A., Neale, P.A., Leusch, F.D.L., 2017. Impact of microplastic beads and fibers on waterflea (Ceriodaphnia dubia) survival, growth, and reproduction: implications of single and mixture exposures. Environ. Sci. Technol. 51, 13397–13406. https://doi.org/10.1021/acs.est.7b03574.